FORMATION OF DOUBLET CRATERS AND HERRINGBONE STRUCTURES: 3D HYDROCODE MODELING. J. D. Kendall[1,2] and N. E. Petro[1], [1]NASA Goddard Space Flight Center, 8800 Greenbelt Rd, Greenbelt, MD 20771 [2]University of Maryland, Baltimore County, Center for Space Sciences and Technology, 1000 Hilltop Circle, Baltimore, MD 21250 (jordan.d.kendall@nasa.gov).

Introduction: The simultaneous impact of two or more objects at close distances often leads to the formation of doublet craters, in which two craters imprint upon each other to form unique patterns such as a dumbbell shape, asymmetric elliptical crater, or distinctive herringbone structures [1,2,3]. With the aid of a three-dimensional (3D) hydrocode, we are able to explore the crater formation from multiple impacts, the timing and emplacement of ejecta, and the formation of V-shaped ridges (so-called herringbone structures). The modeling results align well with previously produced laboratory experiments and observations made during the Apollo missions [2,3].

Craters cover the lunar surface due to meteorites striking the surface and creating primary craters. However, ejected material from these craters also forms secondary craters. The preponderance of secondary craters statistically leads to the occurrence of doublet craters, formed by the near simultaneous impact of two projectiles. Swarms of ejecta strike the planetary body and doublet craters are common within crater ray fields, such as the Copernican secondary craters observed by Apollo 15 [3]. The formation of doublet craters is common on the Moon, Mars, Venus, and the Earth [4]. Such features may be present at the Apollo 17 landing site (e.g. the Victory feature, which may have formed from multiple impact craters).

Here we propose a first step towards a numerical model for secondary doublet craters in the iSALE-3D hydrocode. Previous experiments concluded that the distance between craters and the timing of the uprange and downrange impacts strongly affect the V-shaped ridge angles, whereas the impact velocity plays a negligible role [3]. We base our impact model on the experiments of two projectiles striking a surface a few impactor diameters apart and at speeds (v_{imp} = ~1 km/s) comparable to the boulders that create secondary craters [3]. Previous numerical modeling focuses on the formation of crater rays [5] and primary doublet craters from binary asteroids [4]. Instead, we focus on the craters formed from secondary impacts.

Methods: We simulate the impact and ejected material with the iSALE-3D, an impact shock physics hydrocode capable of three-dimensional (3D) simulations [6,7]. Our model Moon consists of a flat half-space dunite target surface with a surface gravity of 1.62 m/s^2. For our model, dunite serves as a proxy for the Moon's bulk mantle composition [8], and the equation of state is well defined within the iSALE ANEOS library. The impactors, two homogeneous spheres of dunite, collide with the Moon at 1 km/s [3]. For simplicity, we choose dunite for the impactors to minimize the computation time. We vary impact angle between 45° and 90°, and we use an impactor diameter of 0.5 km.

Ejecta tracking. We place Lagrangian tracers, which track the motion of a parcel of material through the Eulerian mesh, in the center of each cell of the simulation space. We treat these tracers as proxies for the ejected mass from the impact, with each tracer representing a volume of 0.015625 km^3 (determined by the cell width, d_0, of the simulation, i.e. 0.25 km). We track the tracer trajectories and determine the locations where they ballistically emplace onto the lunar surface.

Topography Calculation. We calculate the topography by finding the uppermost cell with material inside each vertical cell column. This gives the height above or below the initial surface for the boundary between solid material and vacuum. When the ejecta curtain expands, we determine the topography value along the ejecta curtain rather than the surface beneath. This method allows us to look at the opening craters and ejecta curtains as they interact during transient crater formation.

Figure 1. Profile view of two 0.5 km dunite asteroids striking a dunite lunar surface at 45° and 1 km/s. The downrange direction is to the left. The dark grey isosurface represents the interface between the uppermost surface material and vacuum. The coarse grid in the background provides a scale of one projectile radi-

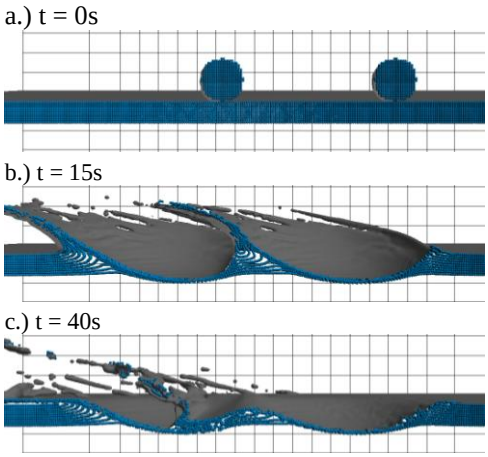

us (0.25 km). The blue spheres symbolize tracers initially along the plane of impact.

Results: As the craters begin to open (Fig. 1), asymmetries form in the crater volume and ejecta curtain due to the downrange momentum. After 15 seconds, the ejecta curtain originating from the right crater interacts with the uprange ejecta of the left crater (Fig. 1b). This interaction hinders the growth of the right crater and causes the ejecta curtain to lose momentum below the surface at the center of the two craters. After 40 seconds, the ejecta from the right crater land within the left crater (Fig. 1c). The infill leads to a smaller crater depth inside the left crater. The interference between the ejecta curtains and subsequent momentum exchange hinders the evolution of the right crater's ejecta, causing different ejecta blanket thickness.

We explore the final crater morphology for varying impactor angle and separation in Fig. 2. Each impact involves two 500 m diameter impactors striking at 1 km/s. The smaller separation distance of 1 km for 2a and 2b result in more crater overlap and thus form elliptical craters. Additionally, the craters exhibit ridge-like structures astride the craters, similar to herringbone structures [2,3]. From each simulation, we are able to determine the crater dimensions, maximum ejection depth, depth of ridge material, and angle between ridges.

Conclusion: The provenance of the ejecta is primarily along a perpendicular line that bisects the points of impact of each projectile. The oblique impact causes an infill of ejecta from the uprange crater into the downrange crater (Fig. 1, 2). This implies the downrange crater is 100 m shallower than the uprange crater. Therefore, the depth of long elliptical craters or those formed as a doublet crater give insight into the direction of the impact, impact angle, and impactor shape. The infill volume depends upon the impact angle, as highly oblique impacts focus additional momentum downrange. The separation of the impactors also determines the location of the uprange crater relative to the downrange crater's ejecta curtain thickness and thus the infill thickness. From this model, we gain additional understanding of the secondary craters that form from near simultaneous impacts of multiple objects, as well as the overlapping ejecta curtains and possible applications to unique craters that have not yet been formally explained (such as the Victory feature in the Taurus-Littrow valley).

Acknowledgements: We give special thanks to the developers of iSALE: Kai Wünnemann, Tom Davison, Gareth Collins, Dirk Elbeshausen, H.J. Melosh, and Boris Ivanov.

References: [1] Oberbeck, V. R., Morrison, R. H., and Wedekind, J. (1972). Apollo 16 Preliminary Science Report, NASA SP-315, Part K, pp. 29-56. [2] Oberbeck, V. R., Morrison, R. H. (1973), Apollo 17 Preliminary Science Report, NASA SP. [3] Oberbeck, V. R., Morrison, R. H. (1973), LPS 1, pp. 107-123. [4] Miljkovic et al., 2013. [5] Shuvalov, 2012 [6] Elbeshausen, D. et al. (2009) *Icarus*, 204, 716-731. [7] Elbeshausen D. and Wünnemann K. (2011) *Proc. 11th Hyper. Imp. Symp.*[8] Pierazzo et al., 1997.

a.) 500m, 30°, 1 km/s, no delay, 1 km separation

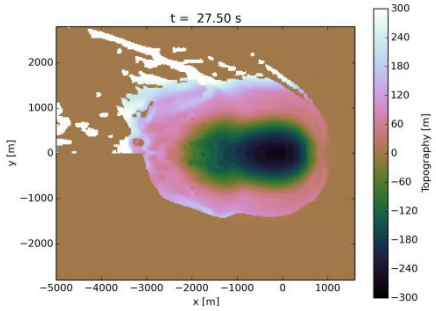

b.) 500m, 45°, 1 km/s, 1s offset, 1 km separation

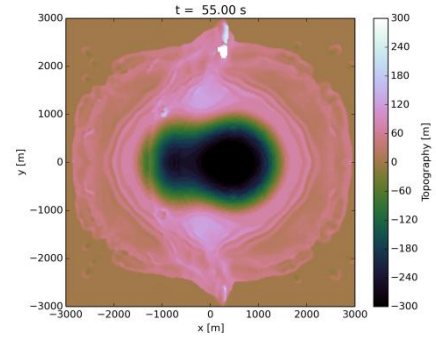

c.) 500m, 60°, 1 km/s, no delay, 2 km separation

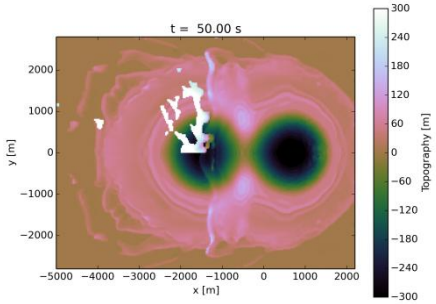

Figure 2: Here we illustrate three impact scenarios. The brown represents the initial surface location at 0 m. The direction of impact is to the left of the image, bisecting the craters at the y = 0 m plane. In the top half panel of each image, we include the remaining ejecta curtain and remove it in the bottom panel. In combination, the two panels give a better view of the top and bottom parts of the ejecta curtain and the opening craters. In Fig 2b and 2c, we note the higher topography ridges that form transverse to the direction of impact.